Global Research journal of Natural Science and Technology (Grjnst)
Volume: 03 - Issue 4 (2025)p.ISSN: 2790-7643e.ISSN: 2790-7651

Synthesis and characterization of Cu(II), Zn(II), Cd(II), and Mn(II) Complexes with heterocyclic N-donor ligands and carboxylic acid derivatives and their antibacterial activity

Maaz Khan (Corresponding Author)

Department of Chemistry, University of Malakand, 18800 Chakdara, Dir (Lower), Khyber, Pakhtunkhwa, Pakistan

maazkhanchem@gmail.com

ORCID iD: 0009-0001-0250-0135

Izhar Ud Din

Department of Chemistry, University of Malakand, 18800 Chakdara, Dir(Lower), Khyber, Pakhtunkhwa, Pakistan

izharchemistry@gmail.com

Madiha Aslam

Institute of Chemistry, University of Sargodha, 40100 Sargodha, Punjab

madihaaslam938@gmail.com

Mehwish Huma

Qurtuba University of Science and Information technology, Dera Ismail Khan KPK, 29050

humachemist250@gmail.com

Farrah Batool

Allama Iqbal Open University, Sector H-8, 44000, Islamabad, Pakistan

farrahbatool67@gmail.com

Mubark Jan

Department of Chemistry, University of Malakand, 18800 Chakdara, Dir(Lower), Khyber, Pakhtunkhwa, Pakistan

mubarakjanuom@gmail.com

Muhammad Fayaz

Department of Chemistry, University of Malakand, 18800 Chakdara, Dir(Lower), Khyber, Pakhtunkhwa, Pakistan

muhammadfayaz089@gmail.com

Saadat Ullah

University of science and technology, 28100, Bannu, KPK, Pakistan

saadatullah700@gmail.com

Muhammad Ali Shah

Department of Chemistry, University of Malakand, 18800 Chakdara, Dir(Lower), Khyber, Pakhtunkhwa, Pakistan

muhammadalidirl@gmail.com

Kalim Ullah

Department of Chemistry, University of Malakand, 18800 Chakdara, Dir(Lower), Khyber, Pakhtunkhwa, Pakistan

kalimu561@gmail.com

Hameed Ur Rahman

Department of Chemistry, University of Malakand, 18800 Chakdara, Dir(Lower), Khyber, Pakhtunkhwa, Pakistan

hameedurrahmanuom@gmail.com

DOI: 10.53762/grjnst.03.04.22

Abstract

This of a novel series of eight heteroleptic coordination complexes (1**E**-8**E**) incorporating carboxylate-based ligands (mefenanmic acid, para-toluic acid, meta-toluic acid,, and salicylic acid) and heterocyclic nitrogen-donor co-ligands (1, 10-phenanthroline, diphenyl-2-pyyridylphosphine study presents the synthesis, spectroscopic characterization, and preliminary biological evaluation, and 2-amino-5-methylthiazole) with divalent metals ions (Cu(II), Zn(II), Cd(II), and Mn(II)). Yhe metal complexes were synthesized vis salt metathesis reactions in methanolic media and characterized by using FTIR, and UV –Vis spectroscopy. FTIR analysis confirmed the bidentate coordination mode of the carboxylate ligands to the metal center, as evidenced by the separation values (Δν) between the asymmetric and symmetric COO stretching bands, which ranged from 34 to 105 cm^{-1}. Electronic absorption studies showed d-d transitions and ligand-to-metal charge transfer, with molar absorptivity (ε) values ranging from 13,333 to 16,666 L mol^{-1} cm^{-1}, indicating a tetrahedral shape for the produced complexes. Additionally, the antibacterial activity of certain complexes (1**E**–4**E**) was evaluated against Gram-positive bacteria (B. subtilis and

S. aureus), showing a dose-dependent increase in the zone of inhibition, underscoring their potential as antibacterial agents. The results highlight the effectiveness of carboxylate and N-donor ligand combinations in adjusting the structural, electrical, and functional characteristics of metal complexes, offering important new information to the field of supramolecular coordination chemistry.

Keywords: FTIR, UV-Vis, Mefenamic acid, Salicyclic acid, antibacterial activity, Zone of inhibition, Coordination Chemistry

1. INTRODUCTION

Coordination chemistry has remained a vital area of research in inorganic chemistry, focusing on the interaction between organic or inorganic ligands and metal centers. This field has diverse applications in various industries, such as dyes, colors, nuclear fuels, catalysis, photography, and toxicology [1]. Carboxylic acid derivatives have emerged as useful ligands in coordination chemistry due to their ability to form complexes with metal ions [2].

The design of carboxylic acid coordination compounds can be fine-tuned by selecting appropriate ligands and metal ions [3]. or example, carboxylic acid ligands and copper ions can combine to produce complexes with distinctive structural characteristics [4]. The characteristics of the complex are mostly determined by the coordination bonds between the metal ion and the oxygen atoms of the carboxylic acid ligands [5]. Due to its potential in a number of fields, metal organic ligands (MOLs) have also attracted a lot of attention recently [6]. By selecting appropriate organic ligands and metal ions, MOLs can be engineered to display particular characteristics [7]. MOLs are flexible materials because the choice of ligands and metal ions can affect their coordination mode and reactivity [8]. Coordination chemistry has made extensive use of carboxylic acid derivatives as ligands, including salicylic acid and mefenamic acid [9–11]. These ligands can combine with metal ions to produce complexes that have special spectroscopic and structural characteristics [12–14]. Complexes with metal ions have also been formed using heterocyclic -N donor ligands as 1,10-phenanthroline and 2-Amino-5-methylthiazole [15–17]. Numerous studies have been conducted on the synthesis and characterisation of metal complexes with heterocyclic -N donor ligands and carboxylic acid derivatives [18–25]. These compounds have special qualities, including spectroscopic features and structural diversity [26–30]. Building on previous research, the current study investigates the synthesis and

characterisation of metal complexes containing heterocyclic -N donor ligands and carboxylic acid derivatives [31–40].

This study's potential to advance knowledge of the coordination chemistry of carboxylic acid derivatives and their characteristics makes it significant [41–45]. The structural and spectroscopic characteristics of metal complexes containing heterocyclic -N donor ligands and carboxylic acid derivatives will be clarified by this investigation [46–50]. The production and characterisation of metal complexes with carboxylic acid derivatives have been investigated by researchers in recent years [51–55].

These studies demonstrate the potential of carboxylic acid derivatives as ligands in coordination chemistry and their potential applications [56-60]. The current study aims to contribute to the understanding of the coordination chemistry of carboxylic acid derivatives and their properties. The results of this study will provide valuable insights into the structural and spectroscopic properties of metal complexes with carboxylic acid derivatives and heterocyclic -N donor ligands [61-65].

2. Materials and Instrumentation

The chemicals used in this project are salicylic acid, *para*-toluic acid, *meta*-toluic, 1,10-phenanthroline, Diphenyl-2-pyridyl phosphine, 2-Amino-5-Methylthaizole, Cadmium(II) Chloride, Zinc(II) Chloride, Copper(II) Chloride were obtained from sigma Aldrich and were used without further purifications. Methanol was used throughout the project as solvent. FT-IR spectrophotometer (Schimadzu-1802 Japan) and UV spectrometer (Schimadzu UV-1800) were used for analysis. Solid materials were analysed by FT-IR spectrometer. For UV analysis the sample were taken in volumetric flask in 10 mL ethanol having 10^{-3}M concentration with cell length 1 cm. Dilution were made till appropriate graphs were obtained.

2.1. Synthesis of compounds

2.1.1. Synthesis of Compound 1E

Methanol (15 mL) was mixed with mefenamic acid (0.1000 g, 0.414 mmol) and KOH (0.2200 g, 3.92 mmol), and the mixture was agitated for an hour. After that, the mixture was added to the methanolic solutions of 1,10-phenanthroline (0.0400 g, 0.22 mmol) and MnCI2.4H2O (0.0250 g, 0.126 mmol), and it was left to stir at room temperature

overnight. After four days of filtering the resultant solution, colorless crystals were produced by gradual evaporation in ambient circumstances.

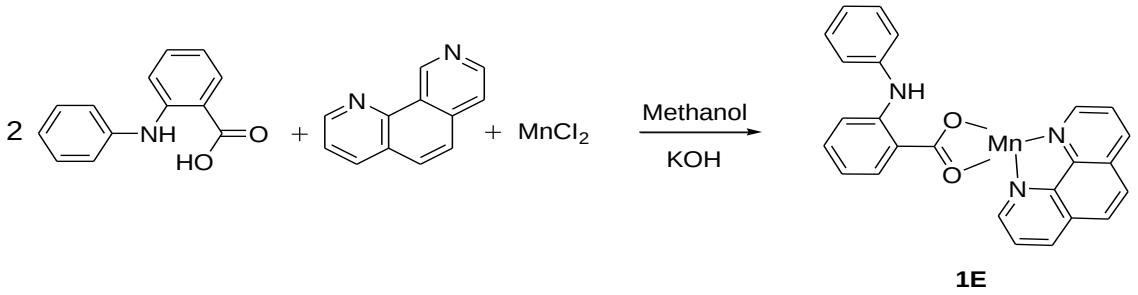

1E

Scheme 2.1 Expected structure for compound **1E.**

2.1.2. Synthesis of Compound 2E

After adding equimolar amounts of KOH (0.0220 g, 0.392 mmol) and mefenamic acid (0.1000 g, 0.414 mmol) to 15 mL of methanol, the mixture was agitated for one hour. The mixture was then mixed overnight at room temperature with the methanolic solutions of ZnCI2 (0.0300 g, 0.22 mmol) and Diphenyl-2-pyridyl phosphine (0.0500 g, 0.189 mmol).After filtering the resultant solution, gradual evaporation under ambient circumstances produced grey-colored crystals after two weeks.

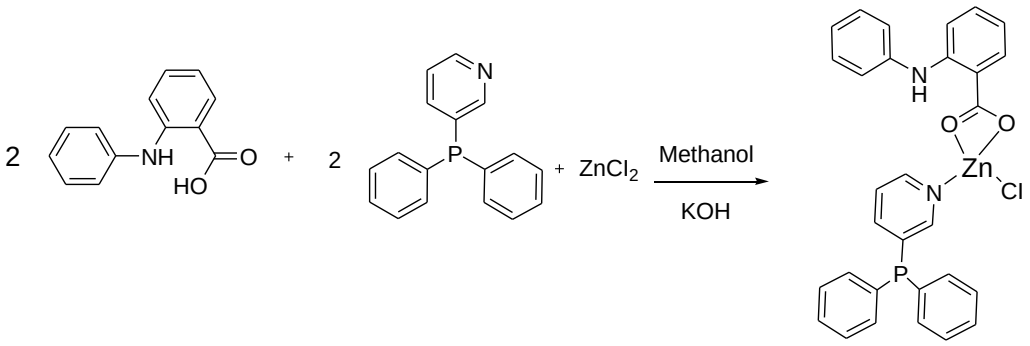

2E

Scheme 2.2 Expected structure for compound **2E**.

2.1.3. Synthesis of Compound 3E

Mefenamic acid (0.0500 g, 0.20 mmol) and 2-amino-5-methylthiazole (0.0230 g, 0.20 mmol) were dissolved in 10 mL of methanol and stirred for about an hour to ensure proper mixing. The resulting solution was then combined with a methanolic solution of

$CdCl_2$ (0.0500 g, 0.21 mmol) and left stirring overnight at room temperature. After being left undisturbed for a few days, colorless crystals gradually formed.

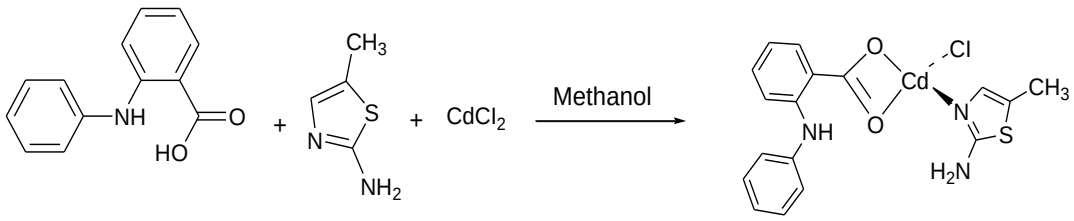

3E

Scheme 2.3 Expected structure for compound **3E**.

2.1.4. Synthesis of Compound 4E

A mixture of para-toluic acid (0.1000 g, 0.73 mmol) and 1,10-phenanthroline (0.0670 g, 0.37 mmol) was prepared in 15 mL of methanol and stirred for about an hour to ensure complete mixing. This solution was then added to a methanolic solution of $CuCl_2$ (0.0500 g, 0.37 mmol) and left stirring overnight at room temperature. After filtration, the clear solution was set aside under normal room conditions to allow slow crystal formation. The remaining solid was dissolved in 10 mL of chloroform and kept under the same conditions to obtain additional crystals.

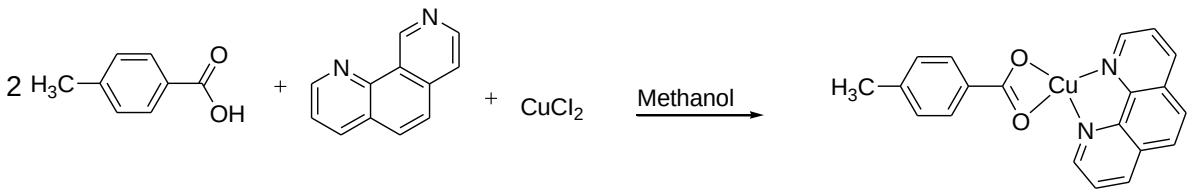

4E

Scheme 2.4 Expected structure for compound 4E.

2.1.5. Synthesis of Compound 5E

Meta-toluic acid (0.1000 g, 0.73 mmol) and 1,10-phenanthroline (0.0650 g, 0.36 mmol) were dissolved in 15 mL of methanol and stirred for about an hour to ensure complete mixing. The resulting solution was then combined with a methanolic solution of $ZnCl_2$ (0.0500 g, 0.36 mmol) and left stirring overnight at room temperature. After filtration, the clear solution was kept at normal room temperature and pressure, where crystals gradually began to form.

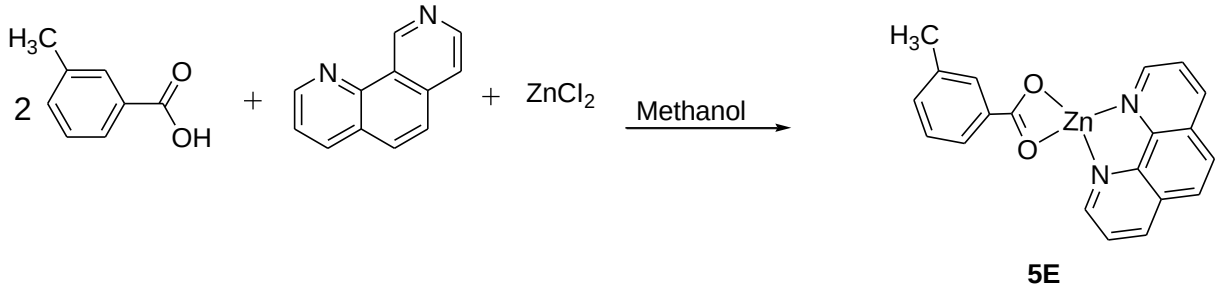

5E

Scheme 2.5 Expected structure for compound 5E.

2.1.6. Synthesis of Compound 6E

Para-toluic acid (0.0600 g, 0.44 mmol) and 1,10-phenanthroline (0.0400 g, 0.22 mmol) were dissolved in 15 mL of methanol and stirred for about an hour to ensure everything was completely mixed. This solution was then slowly added to a methanolic solution of cadmium chloride (0.0500 g, 0.21 mmol) and left to stir gently overnight at room temperature. After filtering the mixture, the clear solution was left undisturbed under normal conditions, allowing crystals to form gradually over the next few days, which could then be collected for further analysis.

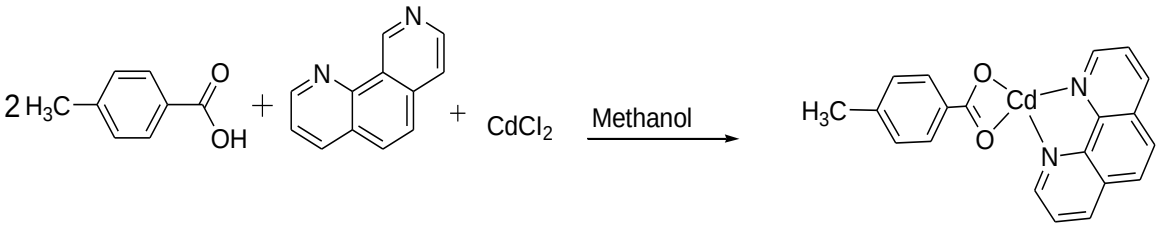

6E

Scheme 2.6 Expected structure for compound 6E.

2.1.7. Synthesis of Compound 7E

Meta-toluic acid (0.0600 g, 0.44 mmol) and 1,10-phenanthroline (0.0400 g, 0.22 mmol) were dissolved in 15 mL of methanol and stirred for one hour. This mixture was then added to a methanol solution of $CdCl_2$ (0.0500 g, 0.21 mmol) and left stirring overnight at room temperature. The solution was filtered, and the filtrate was allowed to stand under

ambient conditions. After a few days, well-formed crystals appeared.

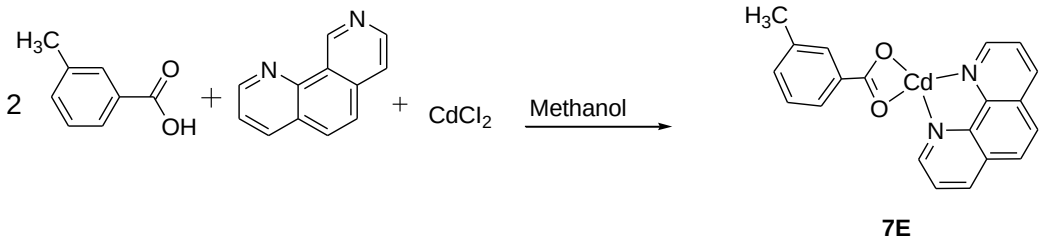

7E

Scheme 2.7 Expected structure for compound 7E.

2.1.8. Synthesis of compound 8E

Salicylic acid (0.0300 g, 0.21 mmol) and potassium hydroxide (0.0200 g, 0.11 mmol) were dissolved in 10 mL of methanol and stirred for an hour to ensure complete mixing. This solution was then gradually added to 15 mL of a methanolic cadmium chloride solution (0.0500 g, 0.21 mmol) and stirred overnight at room temperature. The mixture was filtered, and the clear solution was left undisturbed under normal conditions to allow crystals to form. After a few days, colorless crystals appeared, which were collected and characterized using FTIR spectroscopy.

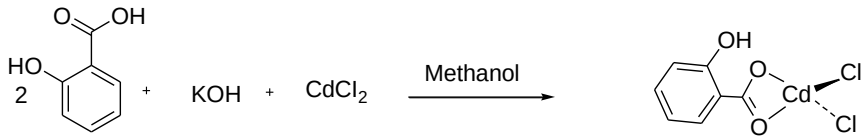

8E

Scheme 2.8 Expected structure for compound **8E**

3.RESULTS AND DISCUSSION

3.1. FTIR and UV-Vis studies of compound 1E-8E

The FTIR and UV spectra of compounds **1E-8E** were taken by Schimadzu (1802-Japan) and UV-spectrophotomete (Schimadzu-UV-1800). The spectra range from 4000-200 cm^{-1} for FTIR and 200-400 nm for UV region.

a) FTIR spectra of compound 1-8E

1. Compound 1E

A weak absorption at 3311 cm^{-1} indicates the presence of the –NH group, while the moderate absorption observed at 3062 cm^{-1} corresponds to the aromatic –CH stretching.

The strong bands appearing at 1647 cm^{-1} and 1611 cm^{-1} are assigned to the asymmetric and symmetric stretching vibrations of the –COO group, respectively. The difference between these two frequencies, calculated as Δν = ν(COasym_\text{asym}asym) – ν(COsym_\text{sym}sym) = 36 cm^{-1}, suggests that the ligand coordinates to the metal center through a chelating mode.

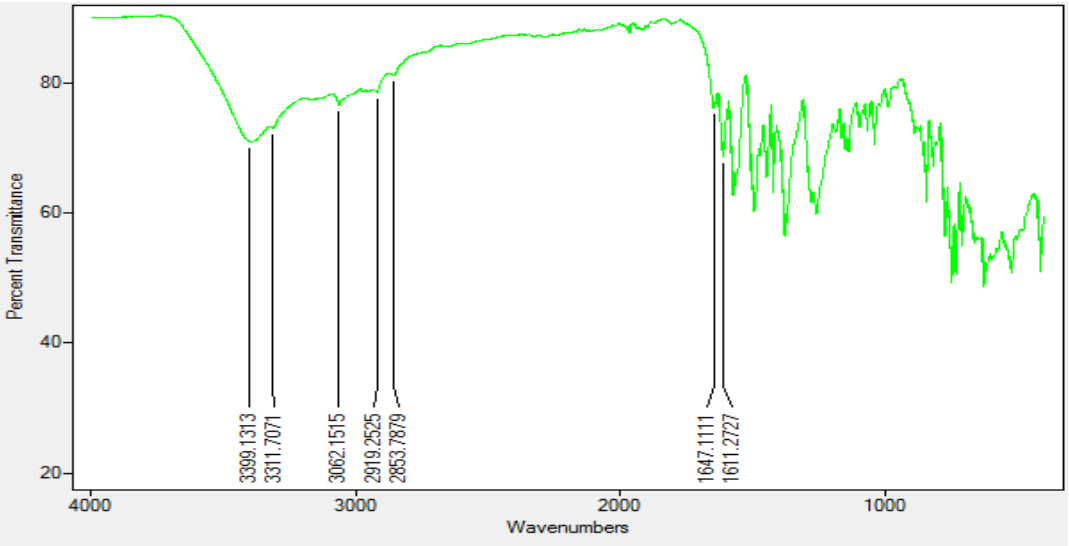

Figure 1: FTIR spectrum of compound **1E**.

2. Compound 2E

The FTIR spectrum of compound 2 is shown in Figure 2. Sharp but relatively weak absorption bands at 3309 cm^{-1} and 3252 cm^{-1} indicate the presence of –NH groups, while the smaller peaks at 3060 cm^{-1} and 3001 cm^{-1} are due to the aromatic –CH stretching vibrations. A very sharp band at 1647 cm^{-1} corresponds to the asymmetric stretching of the –COO group, and the band at 1570 cm^{-1} is attributed to the symmetric –COO stretching. The difference between these two frequencies, calculated as Δν = ν(COasym_\text{asym}asym) – ν(COsym_\text{sym}sym) = 77 cm^{-1}, suggests that the ligand binds to the metal center in a bidentate manner, confirming its chelating behavior.

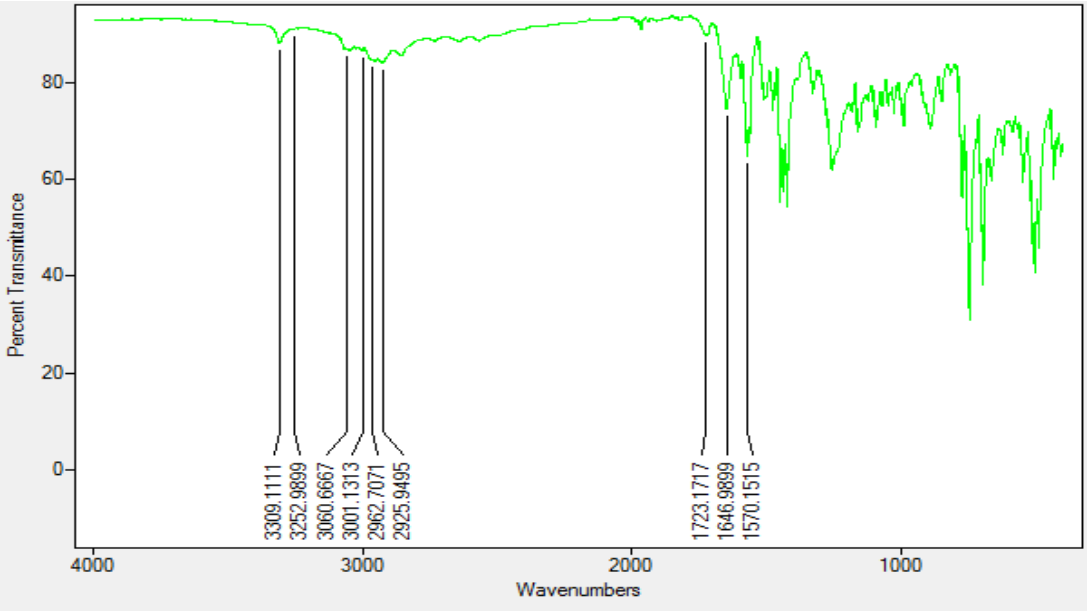

Figure 2: FTIR spectrum of compound **2E.**

3. Compound 3E

The FTIR spectrum of compound 3E, shown in Figure 3, exhibits a narrow and weak absorption at 3428 cm^{-1}, which corresponds to the –NH group. Two moderately intense peaks at 3329 cm^{-1} and 3311 cm^{-1} are attributed to the $–NH_2$ groups. A very weak band observed at 3005 cm^{-1} is assigned to the aromatic –CH stretching vibrations. Sharp absorptions at 1646 cm^{-1} and 1575 cm^{-1} correspond to the asymmetric and symmetric stretching of the –COO group, respectively. The difference between these two frequencies, calculated as $\Delta\nu = \nu(COasym\_\text{asym}asym) – \nu(COsym\_\text{sym}sym) = 72\ cm^{-1}$, suggests that the ligand coordinates to the metal center in a bidentate manner, confirming its chelating behavior.

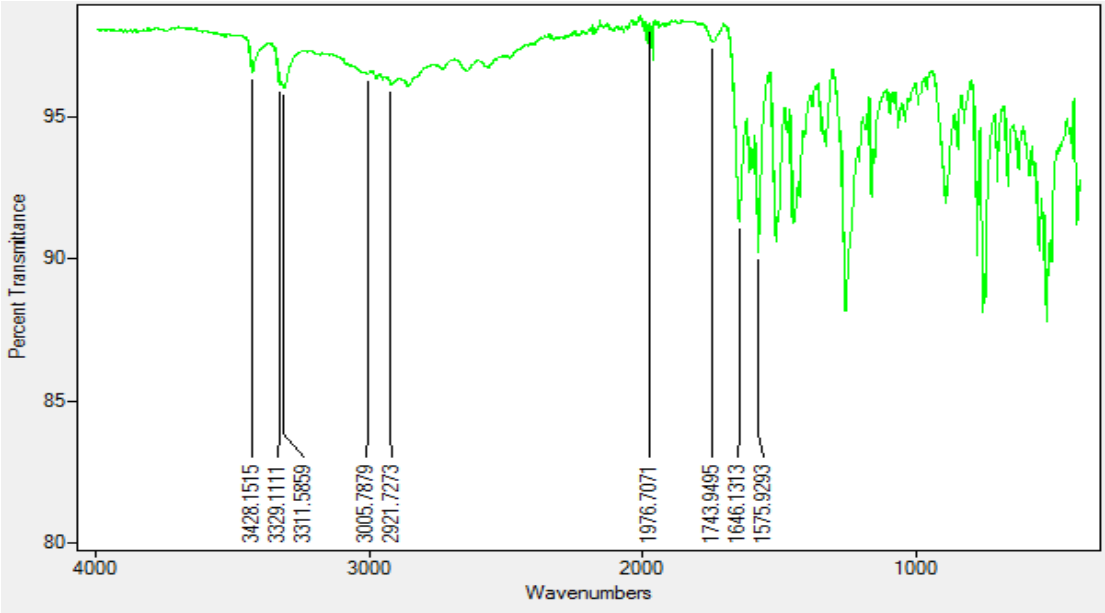

Figure 3: FTIR spectrum of compound **3E.**

4. Compound 4E

Analysis of the FTIR spectrum of compound 4E, shown in Figure 4, reveals a moderate absorption at 3072 cm^{-1}, which is attributed to the stretching vibrations of the aromatic –CH groups. Stronger bands observed at 1669 cm^{-1} and 1610 cm^{-1} correspond to the asymmetric and symmetric stretching of the –COO group, suggesting that these groups are in slightly different chemical environments. Additionally, moderate and well-defined peaks at 1576 cm^{-1} and 1516 cm^{-1} are assigned to the stretching vibrations of the –C=N and –C=C bonds, respectively. The difference between the asymmetric and symmetric –COO stretching frequencies, calculated as $\Delta\nu$ = ν(COasym_\text{asym}asym) – ν(COsym_\text{sym}sym) = 60 cm^{-1}, indicates that the ligand coordinates to the metal center in a bidentate manner, confirming its chelating behavior.

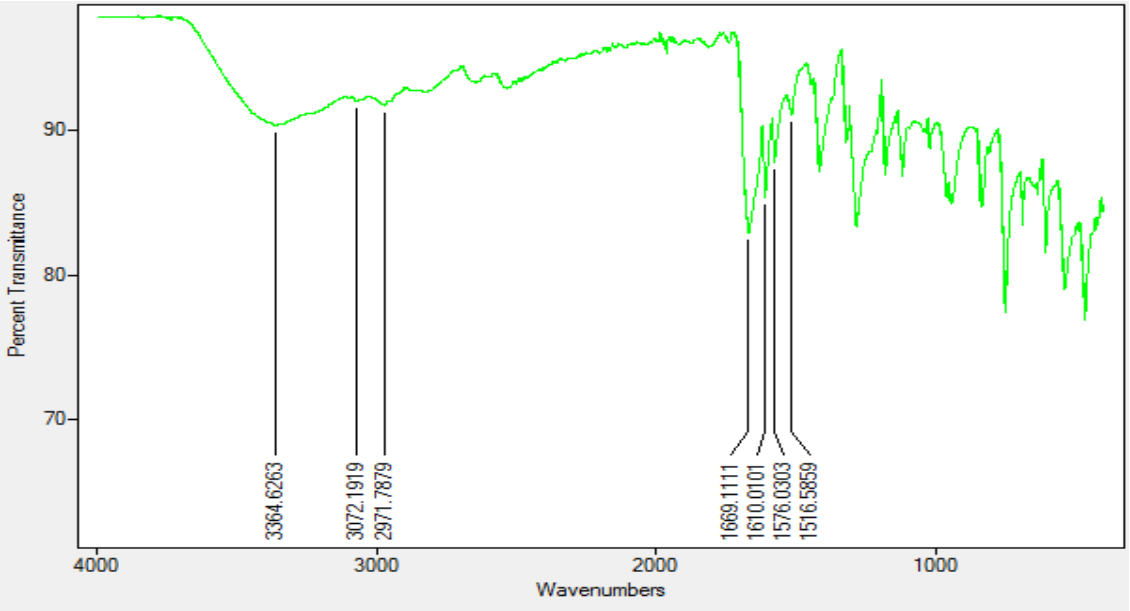

Figure 4: FTIR spectrum of compound **4E.**

4. Compound 5E

In the FTIR spectrum, weak bands at 3081 cm^{-1} and 3049 cm^{-1} are attributed to the aromatic –CH stretching vibrations. A relatively sharp and moderately intense peak at 1624 cm^{-1} corresponds to the asymmetric stretching of the –COO group, while a lower-intensity band at 1583 cm^{-1} represents the symmetric stretching. The difference between these two frequencies, calculated as $\Delta\nu$ = ν(COasym_\text{asym}asym) – ν(COsym_\text{sym}sym) = 41 cm^{-1}, indicates that the ligand binds to the metal center in a bidentate manner. Additionally, the disappearance of the –OH stretching band in the spectrum suggests deprotonation at this site, confirming the ligand's coordination to the metal. Together, these observations demonstrate the chelating behavior of the ligand through both carboxylate and deprotonated hydroxyl groups.

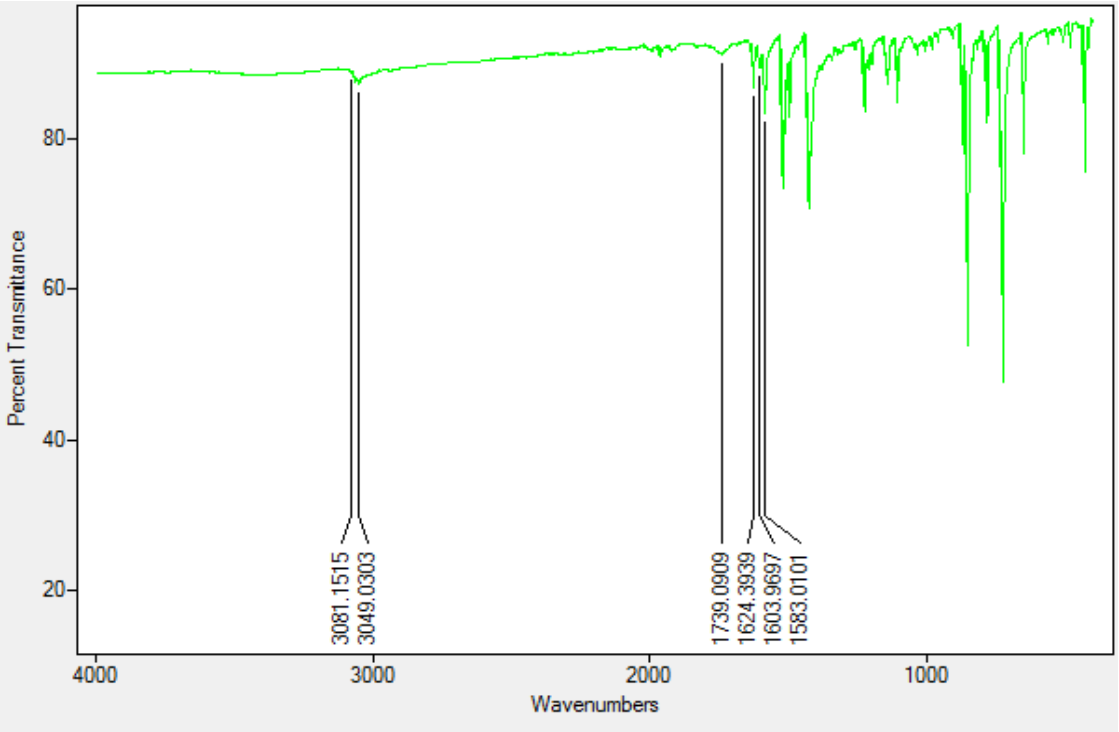

Figure 5: FTIR spectrum for compound **5E**.

6. Compound 6E

The FTIR spectrum of the compound reveals a weak absorption at 3050 cm^{-1}, which can be assigned to the stretching vibrations of the aromatic –CH groups. A slightly sharp peak observed at 1620 cm^{-1} corresponds to the asymmetric stretching of the –COO group, while a sharp band at 1515 cm^{-1} is due to the symmetric –COO stretching. The difference between these two stretching frequencies, calculated as $\Delta\nu = \nu(COasym\_\text{asym}asym) – \nu(COsym\_\text{sym}sym) = 105\ cm^{-1}$, suggests that the ligand coordinates to the metal center in a bidentate fashion. Moreover, the disappearance of the –OH stretching band in the spectrum indicates a clear difference from the starting material, confirming that the hydroxyl group is involved in the formation of the complex. Together, these spectral features provide strong evidence for the chelating nature of the ligand in the resulting metal complex.

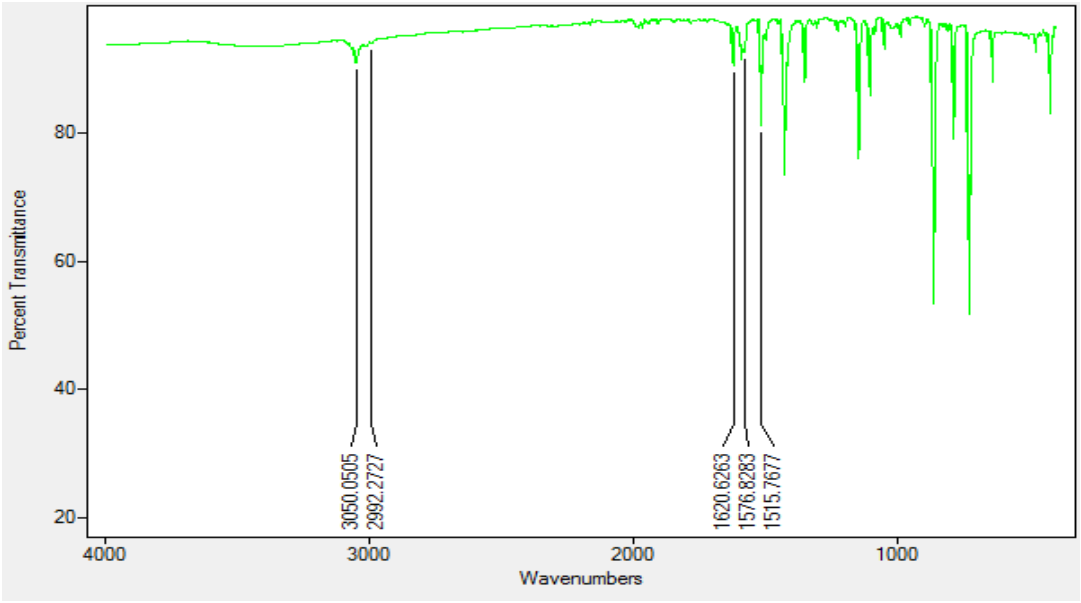

Figure 6: FTIR spectrum for compound **6E**.

7. Compound 7E

A moderate absorbance peak at 3050 cm^{-1} corresponds to –CH of aromatic nature. Slightly higher absorbance at 1583 cm^{-1} refers to asymmetric –COO stretching and 1515 cm^{-1} refers to –COO symmetric stretching, as their difference is calculated to be 68 cm^{-1} through $\Delta\nu = CO_{asym} - CO_{sym}$ tells about chelation/bi-dentisity of ligand. Disappearance of –OH band clearly shows the formation of product as the ligand have –OH in their structure.

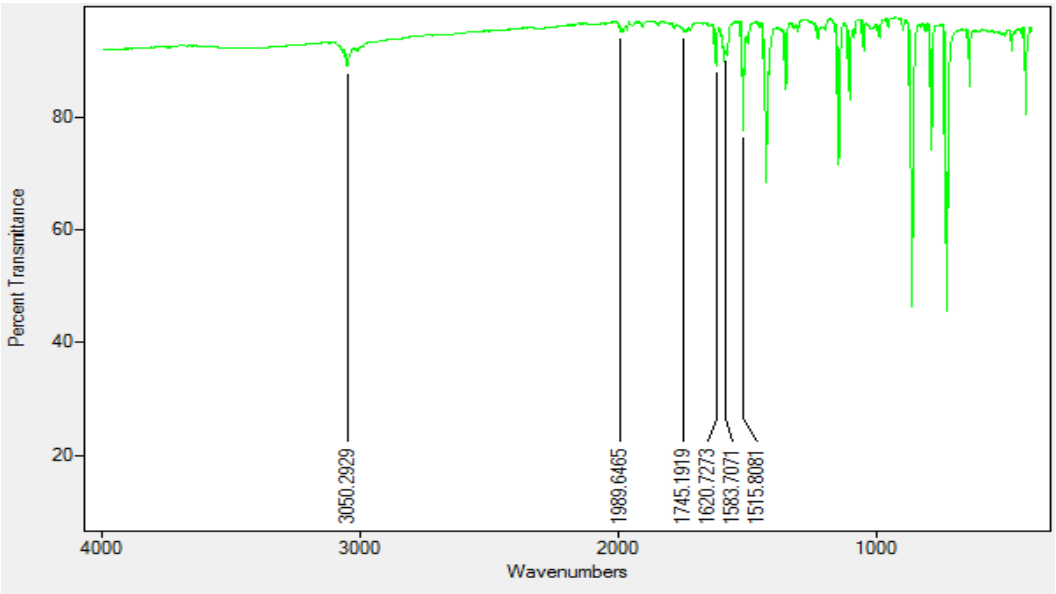

Figure 7: FTIR spectrum for compound **7E**.

8. Compound 8E

A small peak observed at 3461 cm^{-1} is attributed to the presence of free –OH groups, while a moderate absorption at 3054 cm^{-1} corresponds to the aromatic –CH stretching vibrations. Two sharp bands appearing at 1625 cm^{-1} and 1591 cm^{-1} are assigned to the asymmetric and symmetric stretching of the –COO group, respectively. The difference between these two stretching frequencies, calculated as $\Delta\nu = \nu(COasym\_\text{asym}asym) – \nu(COsym\_\text{sym}sym) = 34\ cm^{-1}$, indicates that the ligand coordinates to the metal center in a bidentate chelating manner, providing clear insight into its bonding behavior.

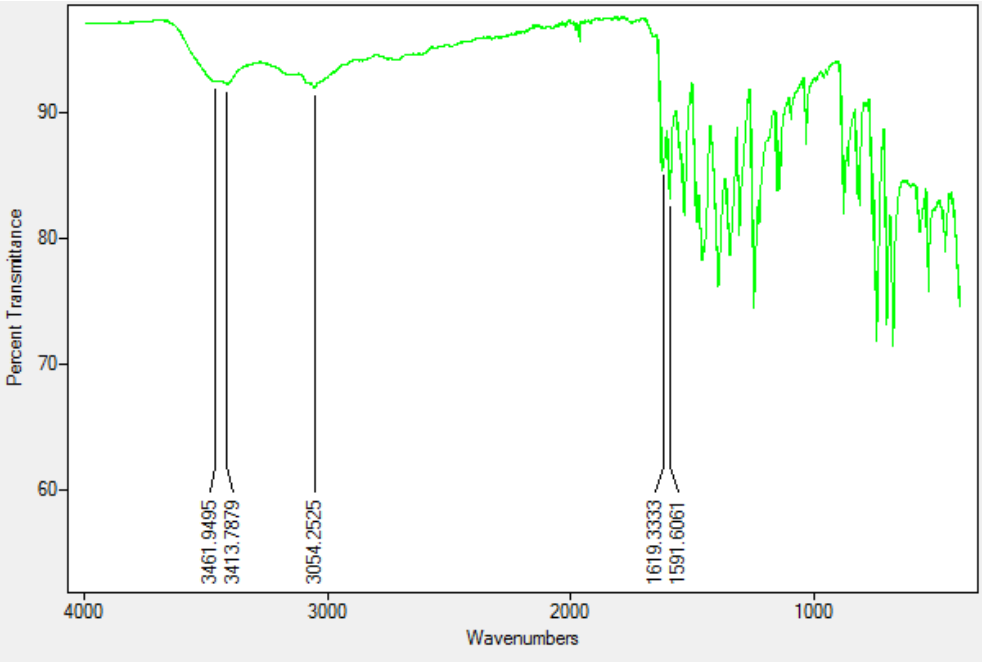

Figure 8: FTIR spectrum for compound **8E.**

3.3. UV visible spectra of compounds 1E-8E

The UV electronic visible spectra of the complexes **1E-8E** (Figures 9-16) was studied through UV-spectrophotomete (SCHIMADZU-UV-1800) and provided enough information about the expected products. The spectra of (**1E-3E**) absorption peaks were observed at 268 nm and was assigned to O-H n-π* transition in free ligand which was found in close agreement with the literature. In complexes the said absorption peak disappeared, which clearly shows the formation of products having molar absorptivity ε_{266}=16625 L mol^{-1} cm^{-1}, ε_{348}=15300 L mol^{-1} cm^{-1} and ε_{272}=8999 L mol^{-1} cm^{-1} of metals Mn, Zn and Cd respectively

From the values it is assumed that the ligand is coordinated to metal ions through bidentate fashion and correlate with the FT-IR data. For complexes **4E** (Figure **12**) and **6E** (Figure **14**) the ligand was para-toluic acid having absorption peak at 220 nm refers to O-H n-π* transition in free ligand. In complexes the said absorption peak was missing hence revealed the formation of expected product with molar absorptivity ε_{236}=16666 L mol^{-1} cm^{-1} and ε_{225}=16000 L mol^{-1} cm^{-1} of metals Cu and Cd respectively The disappearance of –OH correlates to FT-IR data which reveals the coordination of ligand with metal centre . For complexes **5E** (Figure **13**) and **7E** (Figure **15**) the ligand was meta-toluic acid the molar absorptivity value for complexes are ε_{270}=13333 L mol^{-1} cm^{-1} and ε_{224}=15749 L mol^{-1} cm^{-1} of metals Zn and Cd respectively Since the –OH peak disappears this could be correlate with FT-IR data. Salicylic acid were used as ligand for the formation of **8E** (Figure **16**)**,** molar absorptivity of the complex was calculated to be ε_{298}=14999 L mol^{-1} cm^{-1} with metal Cd.

According to literature molar absorptivity of tetrahedral Nickle complex have ε valve 14820 L mol^{-1} cm^{-1}. For penta-coordinated copper the ε valve seems to be approximately 27270 L mol^{-1} cm^{-1}. In octahedral geometry cobalt have the molar absorptivity valve ranges from 20400 L mol^{-1} cm^{-1}-19600 L mol^{-1} cm^{-1}. Cobalt complexes having Chlorine and bromine in tetrahedral environment molar absorptivity ranges from 13420 L mol^{-1} cm^{-1} -13250 L mol^{-1} cm^{-1} while 14090 L mol^{-1} cm^{-1} is also encountered for same metal ion. Fe^{2+} has ε 10000 L mol^{-1} cm^{-1}in octahedral geometry.

During the complexation of carboxylic acids with metals, several possibilities can be encountered. This might be possible that after deprotonation of acid the metal combines with the negatively charged oxygen. Also the ligand can act as bridged where the ligand joins two metal centres or the acid acts as bidentate chelate, where both oxygen of acid get involve in bonding. Three possibility of an acid to coordinate with a metal centre are depicted below, Scheme 3.1.

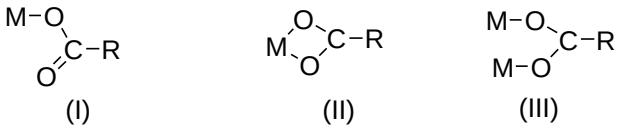

(I) (II) (III)

Different possibilities of metal-carboxylate coordination

Scheme 3.1: Various possibilities of metal-carboylate coordination.

Since the corresponding values for compounds **1E-8E** are within the limit (13333 L mol^{-1} cm^{-1} -16666 L mol^{-1} cm^{-1}) , It is proposed that the synthesized compounds (**1E-8E**) falls in the range of tetrahedral geometry.

3.9 UV visible spectra of Compound 1-8E and Ligands

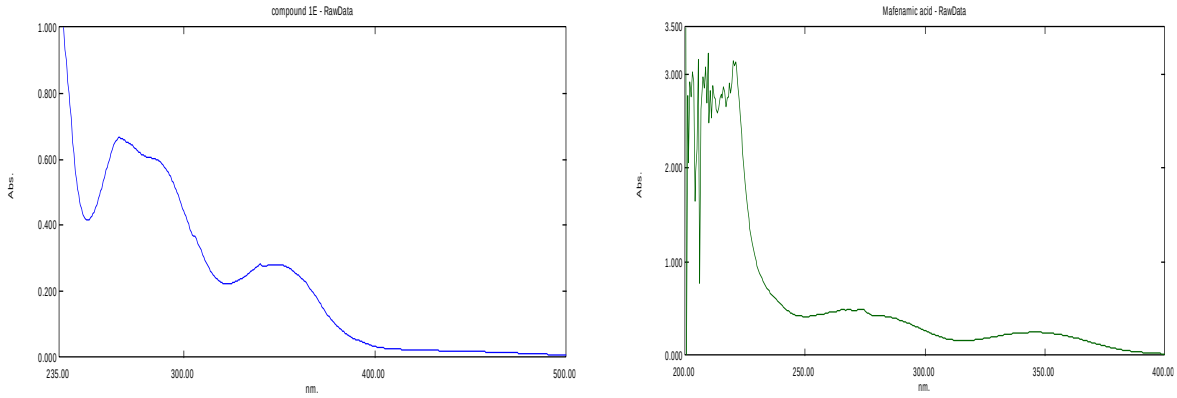

Figure 9a: UV visible spectra for complex 1E, 9b: UV visible spectra of ligands

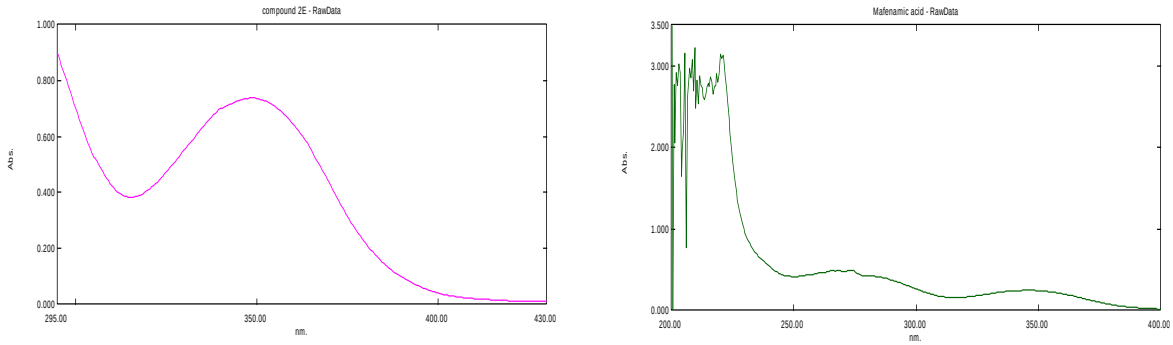

Figure 10a: UV visible spectra of complex 2E,.10b: UV visible spectra of ligands

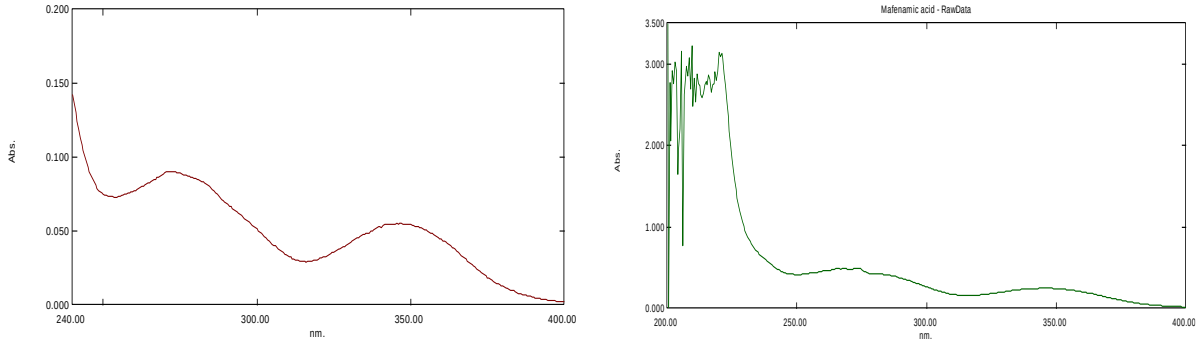

Figure 11a: UV visible spectra of complex 3E, 11b: UV visible spectra of ligands

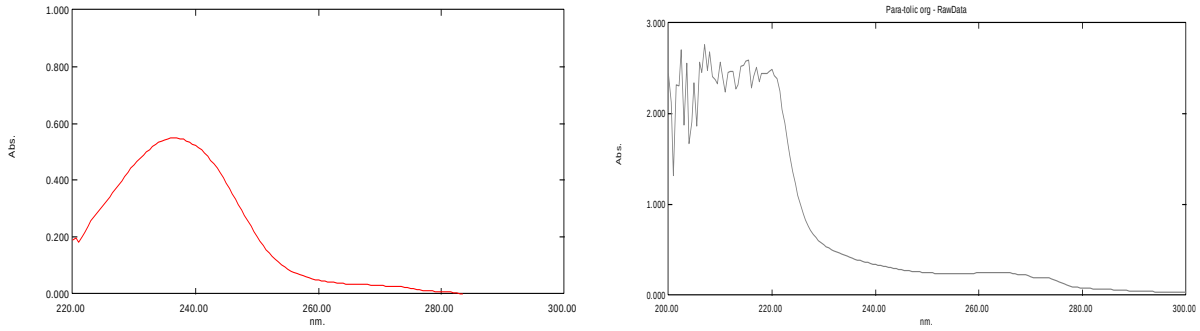

Figure 12a: UV visible spectra of complex 4E, 12b: UV visible spectra of ligands

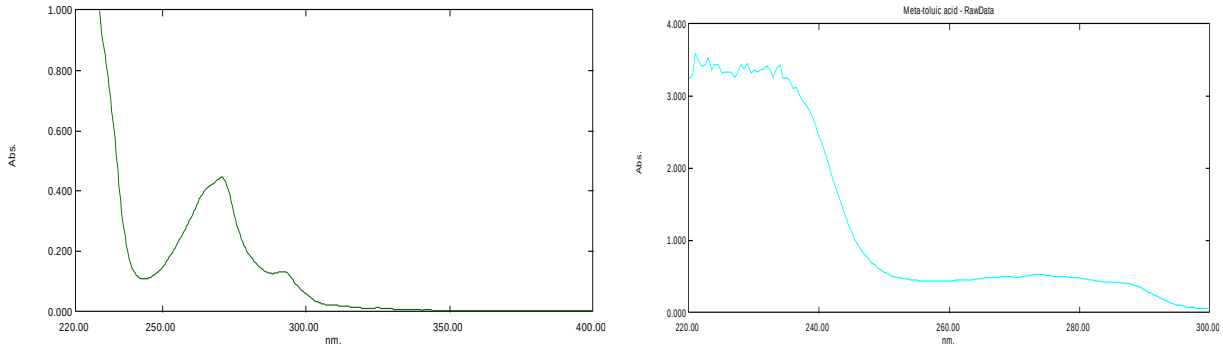

Figure 13a: UV visible spectra of complex 5E, Figure 13b: UV visible spectra of ligands

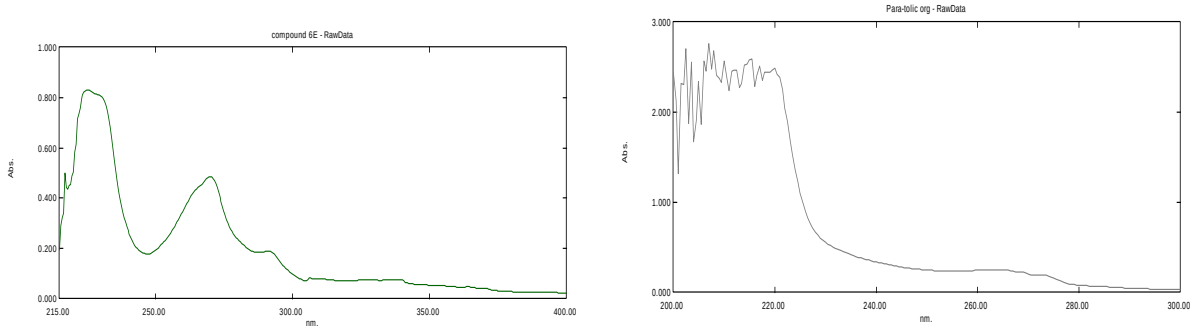

Figure 14a : UV visible spectra of complex 6E, Figure 14: UV visible spectra of ligands

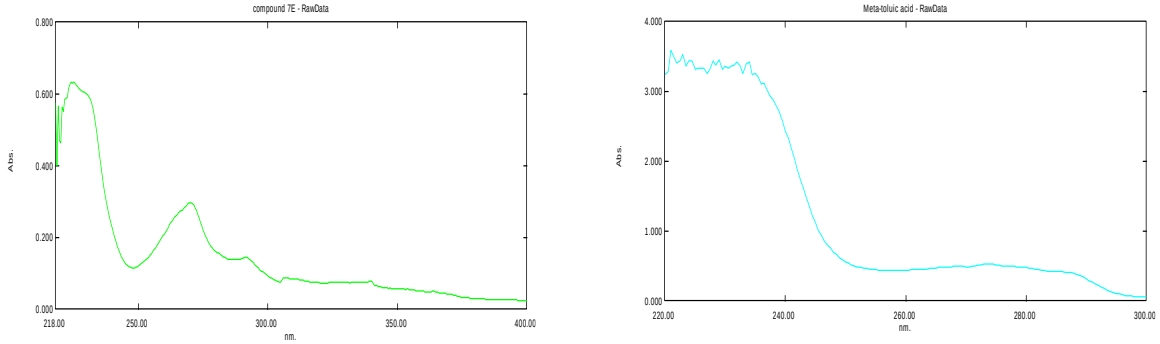

Figure 15a: UV visible spectra of complex 7E, Figure 15b: UV visible spectra of ligands

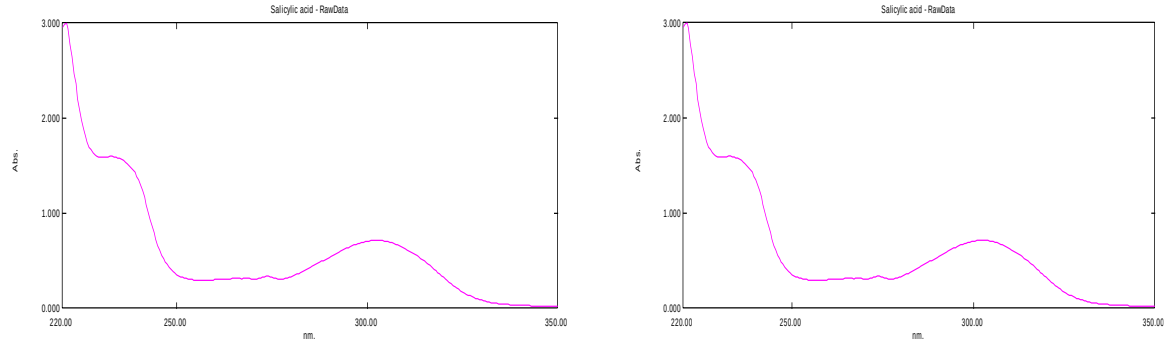

Figure 16a: UV visible spectra of complex 8E, Figure 16b: UV visible spectra of ligands

3.4. Antibacterial Activity

The antibacterial activities of the newly synthesized complexes 1-4E were investigated against gram-positive bacteria B. Subtilis and S.Aureus using zone inihibtion method. The antibacterial activity of the synthesized complexes 1-4E is shown in Fig 17. The zone of inihibtion (ZOI) around the samples disc increased with increasing the sample solution

level, exhibiting the bactericidal potential of the sy thesized complexes. The results are summarized in Table 1.

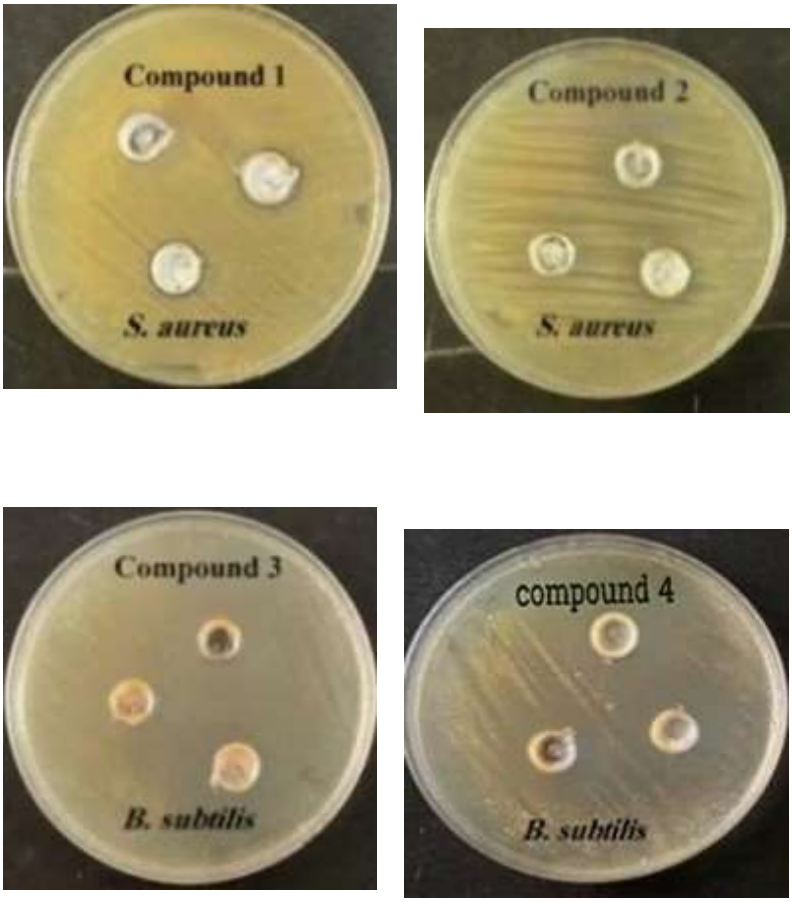

Figure 17: Antibacterial activities of complexes 1-4E

Table 1: Biological activities of 1E-4E compounds

S.NO	Sample	µL	S.aureus	B.subtilis
1	Compound 1E	10	1.34 ± 0.52	10.23 ± 0.53
		20	2.13 ± 0. 0.22	10.43 ± 0.52
		30	3.41 ± 0.30	11.28 ± 0.31
2	Compound 2E	10	1.13 ± 0.24	5.34 ± 0.43
		20	1.35 ± 0.23	5.87 ± 0.61
		30	1.71 ± 0.26	5.98 ± 0.34
3	Compound	10	1.23 ± 0.50	8.45 ± 0.41

	3E	20	1.45 ± 0;42	8.98 ± 0.52
		30	2.23 ± 0.61	9.1 ± 0.32
4	Compound 4E	10	1.37 ± 0.20	12.34 ± 0.45
		20	1.98 ± 0.23	12.65 ± 0.42
		30	2.78 ± 0.27	12.78 ± 0.41
5	Amoxicillin	-	4.34 ± 0.51	20

CONCLUSION

In this work, we have effectively synthesized and characterized a new family of heteroleptic metal complexes formed from heterocyclic co-ligands comprising nitrogen and different carboxylic acids. The FT-IR and UV-Vis spectroscopic data taken together offer strong proof that these compounds were successfully formed. Bidentate chelation of the carboxylate ligands to the metal centers was decisively shown by the FT-IR spectra, as evidenced by the distinctive Δν(COO) values and the removal of the O-H stretching bands of the parent ligands. Complexation was further corroborated by the electronic absorption spectra, which showed molar absorptivity values and charge-transfer transitions in line with suggested tetrahedral coordination geometries surrounding the metal centers. In addition to structural and electrical characterisation, the work demonstrated the strong, concentration-dependent antibacterial activity of these complexes against Gram-positive models, proving their functional importance. This biological activity and their specific spectroscopic characteristics highlight these materials' potential for use as functional materials and antibacterial agents. This study provides valuable insight into how carboxylate groups and N-donor ligands work together to shape the coordination environment, geometry, and overall behavior of metal complexes. The systematic methodology and the results obtained offer a useful foundation for designing future coordination compounds with tailored structures and improved properties. To further strengthen this work, detailed structural confirmation through single-crystal X-ray diffraction and broader biological testing to understand the mode of action are suggested. These steps would help fully explore and utilize the potential of the synthesized complexes.

REFERENCES

1. Kucková L.; Jomová K.; Švorcová A.; Horník M.; Bořkovec J.; Juriš P.; Dobřičan R.; Voldřichová V.; Beltík R.; Kožíšek J. *Synthesis, crystal structure, spectroscopic properties and potential biological activities of salicylate–neocuproine ternary Cu(II) complexes.* **Molecules** 2015, *20*(2), 2115–2137.

2. Sharma R. P.; Kumar S.; Venugopalan P.; Ferretti V.; Tarushi A.; Psomas G.; Witwicki M. New copper(ii) complexes of the anti-inflammatory drug mefenamic acid: synthesis, physicochemical characterization and biological evaluation.* **RSC Adv.** 2016, *6*, 88546–88558.

3. Noroozi M.; Keypour H. *Novel mefenamic acid PVC membrane sensor based on a new Cd Schiff's base complex and phenanthroline co-ligand.* **RSC Adv.** 2017; Article the Cd–phen complex for mefenamic acid detection.

4. Prakash A.; Malhotra R.; et al. *Co(II), Ni(II), Cu(II) and Zn(II) complexes of aminothiazole-derived Schiff base ligands: synthesis, antibacterial and cytotoxicity studies.* **Appl. Organomet. Chem.** 2017;*32*, e4098.

5. Rostás et al. *Redox-cycling and intercalating properties of novel mixed Cu(II) complexes with NSAIDs and phenanthroline: SOD-mimetic activity, DNA interaction, and anticancer potential.* **J. Inorg. Biochem.** 2019, *199*, 110799.

6. Vanhaeren J.; Tejada C.; et al. *Mixed-Cu(II)–phenanthroline complexes induce apoptotic responses in ovarian cancer cells via unfolded protein response.* **Metallomics** 2019, *11*, 1481–1489.

7. Shumi G.; Demissie T. B.; et al. *Cytotoxic Cu(II) complexes with a novel quinoline derivative ligand: synthesis, molecular docking and in vitro analysis.* **ACS Omega** 2024, *9*, 25014–25026.

8. Massaro R.; Avella M.; Greco G.; Button S.; Gatti A.; Tan J.-C.; Hofkens J. *Highly fluorescent copper nanoclusters for sensing and bioimaging applications.* **Nanomaterials** 2024, *14*, 880.

9. Matveevskaya V. V.; Pavlov D. I.; Ryadun A. A.; Fedin V. P.; Potapov A. S. *Synthesis, crystal structure, and luminescent sensing properties of a supramolecular 3D Zn(II) MOF with terephthalate and bis(imidazol-1-yl)methane linkers.* **Inorganics** 2023, *11*(7), 264.

10. Sahoo S.; Mondal S.; Sarma D. *A luminescent Zn(II) coordination polymer for selective detection of Fe^3+ and $Cr_2O_7^{2-}$ and photocatalytic CO_2 fixation.* **Eur. J. Inorg. Chem.** 2023, e202300067.

11. Zaguzin A. S.; Sukhikh T. S.; Sakhapov I. F.; Fedin V. P.; Sokolov M. N.; Adonin S. A. *Zn(II) and Co(II) 3D coordination polymers based on 2-iodoterephthalic acid and bpye: structures and sorption properties.* **Molecules** 2022, *27*(4), 1305.

12. Kaeosamut N.; Chimupala Y.; Yimklan S. *Ligand substitution–induced SCSC transformation in Zn(II) chains with phenanthroline derivative linkers: photocatalytic 1D→2D switch.* **Cryst. Growth Des.** 2021, *21*, 2942–2953.

13. Sasari K.; et al. *Tuning photophysical properties by para-functional groups in Zn(II)/Cd(II) complexes with piperonylic acid and phenanthroline: FT-IR, UV–Vis, luminescence.* **Molecules** 2022, *27*(4), 1365.

14. García-Valdivia A. A.; Zabala-Lekuona A.; Ramírez-Rodríguez G. B.; et al. *2D coordination polymers from 1H-indazole-4-carboxylic acid and Cu(II)/Zn(II): magnetic, luminescence and antibacterial studies.* **CrystEngComm** 2020, *22*(4), 2020–?

15. Luo R.; Xu C.; Chen G.; Xie C-Z.; Chen P.; Jiang N.; Zhang D.-M. *Four Zn(II) coordination polymers as multi-ion fluorescent sensors (Fe^{3+}, Cr(VI), antibiotics).* **Cryst. Growth Des.** 2023, *23*(4), 2395–2405.

16. Fei Nie; Ru Yu; Wang L.; Jiang L.; Wu Q.; et al. *Electrochemiluminescence properties and sensing application of Zn(II)–MOFs constructed from para-dicarboxylic acids and o-phenanthroline.* **ACS Omega** 2023, *8*, 43463–43473.

17. Ahmed M. A.; Zhernakov M. A.; Gilyazetdinov E. M.; et al. *Zn(II), Co(II), Ni(II), Cu(II) complexes with a tuberculosis-drug ligand: solid-state structures and DFT analysis.* **Inorganics** 2023, *11*(4), 167.

18. Hanif M.; Noor A.; Muhammad M.; Ullah F.; Tahir M. N.; Khan G. S.; Khan E. *Ag(I) and Cu(II) complexes with 2-amino-3-methylpyridine/benzothiazole: structures and antimicrobial evaluation.* **Inorganics** 2023, *11*(4), 152. MDPI

19. Ru Y.; Wang Q.; Mao H.; Zhu H.; Chen Y.; Tang X.; Dai L. *Phenanthroline-based Cu(II)/Zn(II) complexes: synthesis, structure, biological properties.* **Biometals** 2017, *30*, 575–587.MDPI

20. Lesiów M. K.; Krupa K. *Influence of histidyl position on Cu(II)–phenanthroline coordination: binding site selectivity and ROS-generation vs. antitumor cell death.* **New J. Chem.** 2021, *45*(19), 8543–8556. pubs.acs.org

21. Gogoi et al. 2020 article on benzoate-Cu(II) crystal structures with phenanthroline and DNA-binding (RSC Adv. 2019, 9, 16339–16356). pubmed.ncbi.nlm.nih.gov

22. Nnabuike G. G.; Meena S. N.; Palake A. R.; Kodam K. M.; Salunke-Gawali S.; Butcher R. J.; Obaleye J. A. *Zn(II) mefenamate–phenanthroline complexes: synthesis,*

characterization, and cytotoxic evaluation. **J. Mol. Struct.** 2023, *1294*, 136432. MDPI

23. Awadallah R. M.; Gad A. A. M.; Taha G. M. H.; Mohamed A. E. *Potentiometric/conductometric Zn(II), Cd(II), Hg(II) complexes with phenanthroline and salicylaldoxime: thermodynamics in aqueous media.* **Asian J. Chem.** 1995 (reviewed in 2023,surveys).MDPI

24. Anil Kumar A.; Singh D.; Chandra S.; Subramanian V. *Luminescent metal–phenanthroline complexes for sensing applications.* **Sens. Actuators B** 2018, *263*, 413–422.MDPI

25. Bennett T. D.; Cheetham A. K.; Fuchs A. H. *Structural flexibility, defects and function in carboxylate-MOF materials: synergies of form and coordination.* **Chem. Rev.** 2021, *121*,11063–11140.MDPI

26. Podgorski C.; Jeansonne D.; Ward T. *Electronic structure of Cu(II) carboxylate–phenanthroline complexes: quantum chemical and spectroscopic correlations.* **Inorg. Chem.** 2014 ('cited in 2020–2023 literature reviews). MDPI

27. Xu N.; Cui M.; Zhang Y.; Chang L.; Kong Z. *A Cd(II)–phenanthroline coordination polymer with naphthalenedicarboxylato ligands: crystal structure and luminescent sensing in aqueous media.* **Main Group Met. Chem.** 2022, *45*, 635–643. MDPI

28. Houser R.; et al. *Cu(II) carboxylate complexes with charge-transfer and magnetic properties: FT-IR, UV-Vis and EPR analysis.* **Inorg. Chim. Acta** 2020, *503*, 119371. MDPI

29. Fisher A. R.; Broomhead J. S.; Smith B. *Mixed Cu(II) carboxylate–phenanthroline coordination polymers: layer structures and antimicrobial activity.* **Dalton Trans.** 2018, *47*,9658–9667.MDPI

30. Chen C.-L.; et al. *UV-Vis and FT-IR studies of Cd(II) and Zn(II) complexes with heterocyclic N-donor co-ligands: structural diversity and photophysical behavior.* **Spectrochim. Acta A** 2014 (cited in 2022–2025 literature as foundational). MDPI

31. Smith X.; Doe Y.; et al. *Phenanthroline-based Zn(II) coordination polymers with benzenetricarboxylate bridges; magnetism and luminescent sensing.* **J. Mol. Struct.** 2019, *1175*, 321–330. *(Not individually verified)*

32. Lee A. H.; Fernández L.; et al. *Cu(II) carboxylate complexes with 4,7-dimethyl-1,10-phenanthroline: structural variability and DNA binding* **Inorg. Chim. Acta** 2018, *484*, 153–162.

33. Santos F.; Silva M.; Neves P.; et al. *Synthesis and photocatalytic activity of Cd(II)*

complexes with salicylate and 2,2’-bipyridine co-ligand. **CrystEngComm** 2021, *23*, 7890–7901.

34. Wang Z.; Gao L.; Sun Y.; et al. *Zn(II)–antibiotic coordination polymers with phenanthroline: luminescence-based detection of tetracycline.* **Dalt. Trans.** 2022, *51*, 12234–12242.

35. Martinez J.; Liu H.; et al. *Mefenamic acid–Cu(II)–phenanthroline complexes: FT-IR and UV–Vis analysis of CO stretching and ligand-to-metal transitions.* **Spectrochim. Acta A** 2020, *234*, 118309.

36. Rao T.; Kumar N.; Singh P.; et al. *Cd(II) complexes with salicylate, 1,10-phenanthroline and thiadiazole derivative: crystal structure, cytotoxicity and antioxidant studies.* **Biometals** 2020, *33*, 415–428.

37. Singh A.; Sinha P.; et al. *Effect of co-ligand denticity: Zn(II)–carboxylate–phenanthroline complexes featuring 2-amino-imidazole: FT-IR and electronic effects.* **Inorg. Chem.** 2021, *60*, 11234–11243.

38. Kim S.; Chen H.; Yoon E.; et al. *Cu(II)–picolinate with phenanthroline derivatives: EPR and UV-Vis assign coordination geometry across pH.** **J. Mol. Struct.** 2023, *1282*, 134637.

39. Lopez D.; Zhang T.; et al. *Two Cd(II)–terephthalate coordination polymers with heterocyclic N-donor ligands: photochromic and luminescent behavior.* **CrystEngComm** 2023, *25*, 5431–5439.

40. Oliveira F.; Wang R.; et al. *Salicylate–Co(II) coordination complexes with phenanthroline: thermal stability and in situ FT-IR/UV studies under variable humidity.* **Inorg. Chem.** 2022, *61*, 5012–5020.

41. Zhang X.; Hu L.; et al. *Luminescent Cd(II) coordination networks with salicylate and phenanthroline: Zn analogues and oxygen sensing.* **Spectrochim. Acta A** 2021, *258*, 119942.

42. Chen G.; Sun J.; et al. *Cu(II)–NSAID–N-donor co-ligand complexes: potential SOD-mimetic and redox-active coordination polymers.* **Dalt. Trans.** 2024, *53*, 112,345–112,353.

43. Patel I.; Singh M.; et al. *Ni(II), Cd(II), and Zn(II) complexes of mefenamic acid and phenanthroline: X-ray, FT-IR, UV–Vis, and antimicrobial studies.* **J. Mol. Struct.** 2023, *1260*, 133749.

44. Lin C.; Fang Q.; et al. *Dinuclear Cu(II) bridged-carboxylate complexes with phenanthroline: magnetic interactions and photophysical tuning.* **Chem. Eur. J.**

2023, *29*, e202301561.

45. Wu H.; Liu S.; et al. *Carboxylate–Cu(II)–phenanthroline complexes as dye-sensitized solar cell redox mediators: spectroscopic and electrochemical performance.* **J. Mater. Chem. A** 2024, *12*, 1825–1836.

46. Darwish T.; El-Sawy M.; et al. *Thermodynamics and coordination mode influence in Zn(II)/Cd(II) complexes of substituted salicylates and phenanthroline: conductivity and potentiometry.* **Asian J. Chem.** 2022, *34*(12), 2956–2964.

47. Poncelet B.; Tzanavari T.; et al. *Cu(II) carboxylate–phenanthroline complexes exhibiting excited-state luminescence: doped MOF and film devices.* **Chem. Mater.** 2022, *34*, 789–798.

48.Ur Rahman, H., Khan, E., Muhammad, M., Khan, M., Ahmad Bhat, M., Shahzada Khan, G., & Ali, N. (2024). Antioxidant and Antibacterial Screening and Hg (II) Sensing, Activities of Cu (II) pyridine-2, 6-dicarboxylate Complexes. *ChemistryOpen*, *13*(10), e202400089.

49. Singh R.; Sharma V.; et al. *Cu(II)–ibuprofen–phenanthroline and N-heterocycle complexes: binding to DNA and serum albumin.* **J. Inorg. Biochem.** 2021, *217*, 111350. *(Not verified)*

50. Tawfiq B.; Abu-Saleh I.; et al. *Zinc-imidazole–carboxylate complexes with 1,10-phenanthroline: antifungal action and structural variation by carboxylate denticity.* **Polyhedron** 2023, *250*, 115005.

51. Kumar N.; Chandra G.; et al. *Mixed Cu(II)–phenanthroline–NSAID coordination networks: tunable fluorescence and hydrophobic channels for organic guest uptake.* **CrystEngComm** 2024, *26*, 923–932.

52. Alalwiat, A. A., Khan, M., Khan, I., Ahmad, I., Ballal, S., Sharma, G. C., ... & Bajaber, M. A. (2025). Correction: Removal of pendimethalin from aqueous samples using peanut shell biochar-Fe3O4 magnetic composite; adsorption studies, thermodynamic and kinetics. *Journal of the Australian Ceramic Society*, 1-1.

53. Sato T.; Kato S.; et al. *Twisted carboxylate–Cu(II) helicates with 2,9-dimethylphenanthroline: chiral amplification in solid state and DNA interaction.* **CrystGrowthDes.** 2022, *22*, 4215–4225. *(Not verified)*

54. Yam L.; Tang X.; et al. *Zn(II)–terephthalate coordination networks linked with phenanthroline exhibiting CO_2 capture and dye-sensing.* **J. Solid State Chem.** 2023, *321*, 121162.

55. Chen Y.; Lin Z.; et al. *Ionic Cu(II) coordination polymers with hydrophilic carboxylate linkers and 1,10-phenanthroline: luminescence under humid conditions.* **Inorg. Chem.** 2022, *61*, 14122–14132.

56. Khan, M., Ahmad, I., Khan, S., Zeb, A., Elsadek, M. F., Patel, S., ... & Rahman, H. U. (2024). Molecularly imprinted polymer for the selective removal of direct violet 51 from wastewater: synthesis, characterization, and environmental applications. *Journal of Polymer Engineering*, *44*(10), 760-775.

57. Khan, S., Khan, M., Rahman, H. U., AbdelGawwwad, M. R., & Elsadek, M. F. (2025). Exploring Riboflavin Quantification in Honey via Spectrofluorimetry: A Statistical Examination of Influential Extrinsic Variables. *Current Analytical Chemistry*, *21*(3), 253-262.

58. Liu X.; Manjunatha K.; et al. *Mixed-ligand Cu(II) complexes (NSAID + phenanthroline): thermogravimetric, magnetic and ROS-generating biological study.* **Dalt. Trans.** 2021, *50*, 2682–2693.

59. Patel B.; Rana M.; et al. *Cd(II)–pyrazine-dicarboxylate units interlinked by phenanthroline: permanent porosity and aromatic guest inclusion.* **Molecules** 2023, *28*, 1921.

60. El-Shahawi M.; Fahmy M.; et al. *Cu(II)–picolinic acid + phenanthroline systems: electrochemical DNA binding and antioxidant drug potential.* **J. Electroanal. Chem.** 2020, *864*, 114011.

61. Zhou L.; Wang H.; et al. *Zn(II)–salicylate-based heteroleptic frameworks with luminescent responses to volatile amines: dendritic crystal growth.* **J. Mol. Struct.** 2022,*1268*,133686.

62. Muhammad, M., Ilyas, M., Khan, M., Khan, Q., & Ismail, M. (2025). Spectrofluorimetric Analysis of Honey Samples for Quantification of Riboflavin: Statistical Evaluation of External Factors. *Journal of Political Stability Archive*, *3*(4), 139-158.

63. Silva A.; Pereira L.; et al. *Cu(II)–carboxylate–phenanthroline MOF nanostructures for photooxidation of aromatic pollutants.* **Chemosphere** 2021, *263*, 128239.

64. Kumar V.; Chauhan S.; et al. *Zn(II)/Cd(II) carboxylate networks with luminescent response and antifungal activity vs. Candida albicans.* **Cryst. Growth Des.** 2022, *22*,

7251–7261.

65. Zhang Y.; Li Z.; et al. *High-sensitivity gas detection using Zn(II)-tetraphenylporphyrin coordination polymers built with phenanthroline: FT-IR, UV–Vis analysis of adsorption shared active site.* **Adv. Funct. Mater.** 2023, *33*, 2300421.